

DC-GAIN LAYER-TO-LAYER STABILITY CRITERION IN LASER METAL DEPOSITION PROCESSES

P.M. Sammons, D.A. Bristow, and R.G. Landers

Mechanical and Aerospace Engineering Department
Missouri University of Science and Technology
Rolla, Missouri 65409-0050

REVIEWED

Abstract

In Laser Metal Deposition (LMD), a blown powder metal additive manufacturing process, functional metal parts are fabricated in a layer-by-layer fashion. In addition to the in-layer dynamics, which describe how the process evolves within a given layer, the additive-fabrication property of LMD creates a second set of dynamics which describe how the process evolves from layer-to-layer. While these dynamics, termed layer-to-layer dynamics, are coupled with both the in-layer dynamics and the process operating conditions, they are not widely considered in the modeling, process planning, or process control of LMD operations. Because of this, seemingly valid choices for process parameters can lead to part failure – a phenomenon commonly encountered when undergoing the laborious procedure of tuning a new LMD process. Here, a layer-to-layer stability condition for LMD fabrications is given, based on the shape of the powder catchment efficiency function, which provides insight into the layer-to-layer evolution of LMD processes and can be useful in process planning and control. The stability criterion is evaluated for various operating points, allowing stable and unstable operating regions to be identified. Simulation results are presented showing both stable and unstable layer-to-layer LMD fabrications. The simulated behavior successfully predicts the results seen in both stable and unstable experimental depositions.

Introduction

Laser Metal Deposition (LMD) is an additive manufacturing process in which a laser and a blown metal powder source are used to create functional metal parts in a layer by layer fashion. The LMD process, and additive manufacturing processes in general, are governed by coupled two-dimensional dynamics – the in-layer dynamics, which describe how the process evolves within a given layer, and the layer-to-layer dynamics, which describe how the process evolves from a given layer to subsequent layers. However, LMD processes are typically modeled as purely in-layer processes and the layer-to-layer dynamics are neglected [1,2]. Neglecting the layer-to-layer dynamics in process planning and attempting to control the process can result in failed parts [3]. An example of a failed part is shown in Figure 1.



Figure 1. Photograph of a failed constant process parameter deposition.

Further, without a model of the layer-to-layer dynamics, insight into how the layer-to-layer dynamics cause part failure is impossible rendering process tuning and planning is extremely difficult.

In order to gain insight into how the process evolves in both dimensions, a repetitive process model was developed in [4]. This model captures the dominant in-layer and layer-to-layer dynamics of the process while still retaining a simple structure allowing it to be used for process control design and planning. While the developed model is dynamic in both the in-layer and layer-to-layer domains, knowledge of the process dynamics for particular systems [5] allows for the application of repetitive process control theory to the model to result in a simple expression to determine the layer-to-layer stability, based on the powder catchment efficiency function of the particular LMD process, for a given set of process parameters. The criterion enables the creation of simple, yet informative process maps for determining whether or not a particular set of LMD process parameters will yield a successful build.

Model Description and Preliminaries

Let h_j denote the height profile of a deposition on a given layer j . On each layer, a new molten bead δh_j is deposited on top of the existing height profile h_{j-1} . Mathematically, this height accumulation is described as an integration process in the layer domain,

$$h_j = \delta h_j + h_{j-1} \quad (1)$$

where j is the layer number, h is the height of the part above the substrate (mm), and δh is the bead height, i.e., the incremental amount of material added to the structure (mm). The bead height is given as

$$\delta h_j = b_0^{-1} \zeta f_\mu (d_{s,j} - h_{j-1}) \lambda_j \quad (2)$$

where b_0 is the characteristic bead width (mm) and converts the area of the bead to the height of the bead, ζ is the material specific volume (mm^3/kg), f_μ is the catchment efficiency function, d_s is the distance between the substrate and the cladding head (mm) and a process input, $\lambda = \dot{m}/v$ is the spatial powder flow rate (kg/mm) and the second process input, \dot{m} is the powder flow rate (kg/s), and v is the substrate scan speed (mm/s).

During a typical operation, the two process inputs, spatial flow rate λ and substrate standoff distance d_s , are commanded to be constant for a given layer. These two input signals, in addition to a set of initial conditions, result in a constant addition of material in the height

direction during each layer. The collection of inputs λ_r and $d_{S,r}$, initial condition on the distance between the part and the cladding head $d_{P,0}$, and outputs h_r that satisfy (1) for all j is termed a solution trajectory. Because the solution trajectory describes a nominal operating process and (1) is a nonlinear discrete dynamic equation, the effects of perturbations to the process on the output are analyzed about this trajectory. Along the solution trajectory with $d_{S,j} = d_{S,r}$, the first order linearization of (1) is

$$\bar{h}_j = \kappa_1 \bar{\lambda}_j + [1 - \kappa_2] \bar{h}_{j-1} \quad (3)$$

where κ_1 is the derivative of f with respect to λ and κ_2 is the derivative of f with respect to d_S (or h),

$$\kappa_1 = b_0^{-1} \zeta f_\mu (d_{P,0}) \quad (4)$$

$$\kappa_2 = -2\lambda_r \alpha_{scale} \zeta \frac{(d_{P,0} - \alpha_{center})}{b_0 \alpha_{width}} f_\mu (d_{P,0}) \quad (5)$$

and the incremental variables are defined as $\bar{h}_j = h_j - h_r$ and $\bar{\lambda}_j = \lambda_j - \lambda_r$. Equation (3) is the linear DC-gain model of the LMD process presented in [4] and more details regarding the full derivation of the model, including the dynamics associated with the in-layer domain, can be found there. Of note is that (3) is a dynamic equation purely in the discrete domain j , i.e., the current height is the previous height plus an input. This structure is analogous to a scalar discrete time dynamic equation. Therefore, discrete domain results will be used to develop a criterion for stability in the layer domain.

DC-Gain Layer-to-Layer Stability Criterion

Informally, layer-to-layer stability is essentially analogous to the conventional one-dimensional notion of input-output stability in that it is required that any bounded input result in a bounded output, under some norm. In the context of (3), the formal definition of layer-to-layer stability is as follows.

Definition [5]: The linear repetitive process (3) is said to be *layer-to-layer stable* if there exists real scalars $0 < M_\infty < \infty$ and $\gamma_\infty \in (0,1)$ which, for each constant input $\bar{\lambda}_j = \bar{\lambda}_\infty$ $j \geq 0$, ensure the output sequence $\{\bar{h}_j\}_{j \geq 0}$ satisfies

$$\|\bar{h}_j - \bar{h}_\infty\| \leq M_\infty \gamma_\infty^j \left(\|\bar{h}_0\| + \frac{\|\bar{\lambda}_\infty\|}{1 - \gamma_\infty} \right), j \geq 0 \quad (6)$$

where \bar{h}_∞ is the equilibrium height profile and \bar{h}_0 is the initial height profile.

The definition for layer-to-layer stability requires that the output, in the case of (3) \bar{h}_j , contract asymptotically to a layer-independent final value \bar{h}_∞ . Physically, Definition 1 requires that the error between the actual height of the part h and the reference part height h_r contract asymptotically towards zero each layer. Applying results from both repetitive process control theory and conventional one-dimensional discrete time systems leads to the following theorem.

Theorem 1: The DC-gain LMD process in (3) is layer-to-layer stable if

$$|1 - \kappa_2| < 1. \quad (7)$$

Examining the definition of the linearization constant κ_2 in (5), it is clear that it depends explicitly on the slope of the catchment efficiency function f_μ . Therefore, as stated in Theorem 1, the process is locally layer-to-layer stable if the rate of catchment (the slope of the powder catchment efficiency) is positive with higher rates leading to larger stability regions. Note that while (7) requires both that $0 < \kappa_2 < 2$, in practice $|\kappa_2| < 1$.

Powder Catchment Efficiency Influence on Layer-to-Layer Stability

For a more physical interpretation, consider a structure whose top surface has a notch feature and a powder catchment function which follows the Gaussian shape as illustrated in Figure 3,

$$f_\mu(d_{p,j}) = \frac{\alpha_{scale}}{100} \exp \left[- \left(\frac{(d_{p,j} - \alpha_{center})}{\alpha_{width}} \right)^2 \right] \quad (8)$$

where α_{scale} is the maximum powder catchment efficiency (%), α_{center} is the vertical distance below the nozzle at which maximum powder catchment efficiency occurs (mm), α_{width} is the powder catchment efficiency characteristic width (mm), and $d_{p,j} = d_{s,j} - h_{j-1}$ is distance between the part and the cladding head (mm). In LMD processes, the blown powder ejected by the cladding head is deliberately shaped such that at a focal point an optimal amount of powder reaches the melt pool, resulting in the powder catchment efficiency function f_μ .

In typical LMD processes, the layer-to-layer change in the substrate standoff distance δd_s is a constant amount for each layer based on knowledge of the bead height δh for a given set of process parameters. If the part standoff distance $d_{p,0}$ initially places the melt pool in Region A (the upper pane in Figure 3), the linearization constant κ_2 in (5), which is proportional to the rate of change of powder catchment efficiency with respect to part standoff distance, is positive. That is, the powder catchment efficiency is increasing with respect to increasing part standoff distance. In this case, the depth of the notch feature will reduce because the powder catchment efficiency is inversely proportional to feature height. When the substrate standoff distance is incremented a constant amount, the melt pool again lies in Region A, further reducing the depth of the notch feature. If the multi-layer deposition is continued without operator intervention when the melt pool lies in Region A, evidence of the notch will continue to attenuate from layer to layer until a constant part height is achieved, as illustrated by the layer-domain schematic on

the right hand side of the top pane in Figure 3. Additionally, as the slope of the powder catchment efficiency function increases, the attenuation of the notch feature occurs in fewer layers.

Alternatively, if the part standoff distance $d_{P,0}$ initially places the melt pool in Region B (the lower pane in Figure 3), the linearization constant κ_2 is negative. That is, the powder catchment efficiency is decreasing with respect to increasing part standoff distance. Incrementing the substrate standoff distance a constant amount and repeating the deposition process with the part standoff distance such that the melt pool lies in Region B further amplifies the notch feature. Without operator intervention, the layer-to-layer growth will eventually lead to catastrophic defects in the deposition, as illustrated in the lower pane in Figure 3.

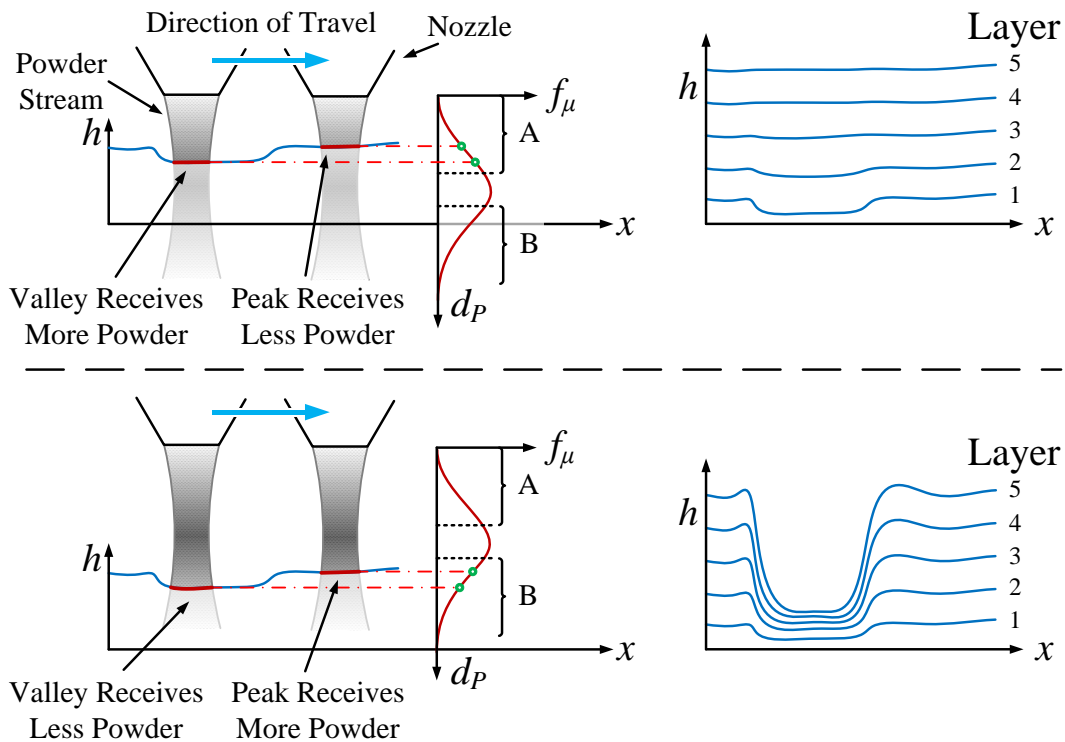


Figure 3. Schematic of deposition process around a stable part standoff distance (Region A, top) and around an unstable part standoff distance (Region B, bottom).

From a control theoretic standpoint, setting the part standoff distance d_P such that the melt pool lies in Region A is an open-loop layer-to-layer stable operating point. Conversely, a part standoff distance such that the melt pool lies in Region B is a layer-to-layer unstable operating point. Additionally, because the DC-gain linear process in (3) is analogous to a 1D discrete time system, the value $|1-\kappa_2|$ is the DC-gain layer-to-layer pole location. As κ_2 approaches unity (higher catchment efficiency slope), the layer-to-layer pole location move towards the origin of the unit disc. This causes the layer-to-layer process speed to increase. This insight follows from discrete-time system theory.

Layer-to-Layer Stability Process Map

Because the DC-gain stability criterion in (7) is explicitly dependent on both the spatial flow rate λ and the part standoff distance, a series of process maps can be constructed to aid the selection of process parameters and operating conditions that result in layer-to-layer stable builds. In previous work by the authors [6] the model presented in the Model Description and Preliminaries section was identified for a well-tuned process on an Optomec MR-7 [7] system using 316 Stainless Steel. The resulting model parameters are given in Table 1.

Table 1. Open-Loop LMD Process Parameters.

| Parameter | Value |
|--|--------------------|
| Characteristic Melt Pool Length, l_0 (mm) | 0.61 |
| Characteristic Melt Shift, δ (mm) | -0.01 |
| Characteristic Melt Pool Width, b_0 (mm) | 0.84 |
| Re-Melt Characteristic Length, l_r (mm) | 1.21 |
| Powder Catchment Scaling, α_{scale} (%) | 16.04 |
| Powder Catchment Center, α_{center} (mm) | 10.57 |
| Powder Catchment Width, α_{width} (mm) | 2.04 |
| Material Specific Volume, ζ (mm ³ /g) | 1.25×10^2 |

The parameters listed in Table 1 are used to calculate the DC-gain stability criterion for various values of part standoff distance d_p , spatial flow rate λ , and bead height δh (mm) – the layer-to-layer change in the total part height. When the stability criterion (7) is violated, the corresponding combination of parameters is deemed an unstable region of the parameter space and is labeled as such. Additionally, because the physical process has limits on how much material can actually be deposited, values of the spatial flow rate which exceed 1×10^{-3} kg/mm are deemed infeasible. Figure 3 shows the resulting process map around the process operating point given by the parameters in Table 1.

In Figure 4, the λ contours represent levels of constant spatial flow rate with zero spatial flow rate occurring in the lower right hand corner of the process map. When spatial flow rate is small, the available values of part standoff and the achievable bead height which yield stable layer-to-layer builds is small, i.e., the length of the contour between $d_p = 5$ mm and $d_p = 10.5$ is shorter for $\lambda = 1 \times 10^{-5}$ kg/mm than that of $\lambda = 5 \times 10^{-5}$ kg/mm. As spatial flow rate increases, the region of stability widens significantly until approximately $\lambda = 1 \times 10^{-4}$ kg/mm when the stability window begins to decrease as the process approaches the unstable region located on the left hand side of the process map.

The second set of contours located on the map indicates constant levels of the stability criterion in (7). The right hand boundary of the stable region indicates the powder catchment center $\alpha_{center} = 10.57$ mm. At this location in the powder catchment efficiency function, there is an inflection point where the slope switches from being positive to being negative. In other words, when the part standoff distance is less than α_{center} the process is operating in Region A as shown in Figure 3. When the part standoff distance is larger than α_{center} the process is operating in Region B in Figure 3. The left hand boundary is a more process-dependent boundary. At this location, the desired bead height and spatial flow rate result in a process which builds too fast and would be coincident with the cladding head if no corrective action was taken, i.e., increase the layer-to-layer increment in substrate standoff distance.

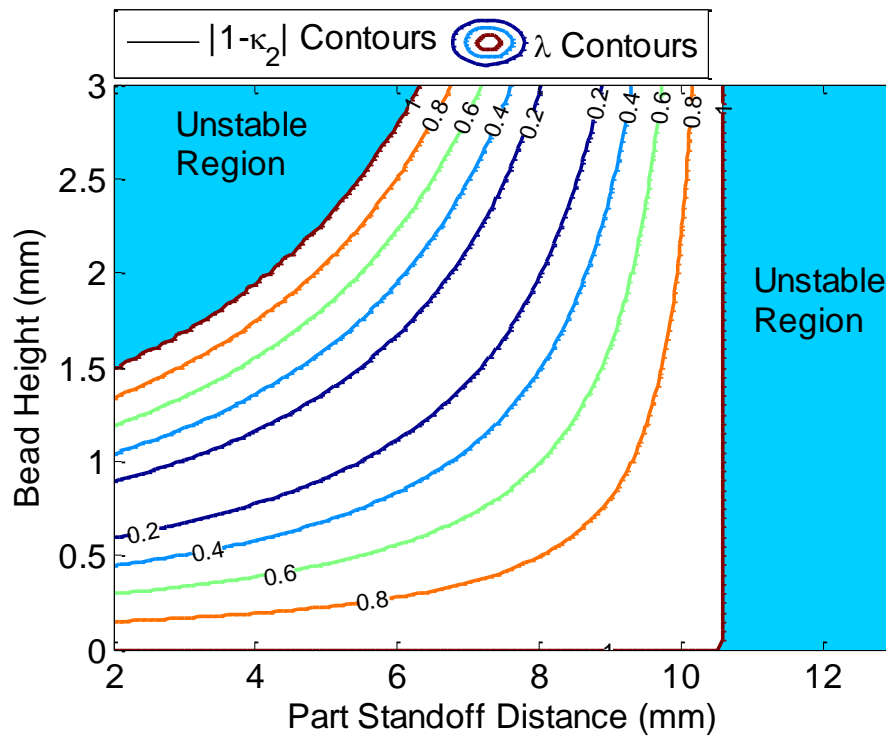


Figure 4. Layer-to-layer stability process map.

Simulation and Experimental Results

To demonstrate the efficacy of the stability criterion and the process map discussed in the previous two sections, two simulations are performed using the full nonlinear dynamic model in [4] and corresponding experimental results are presented. The first simulation and experimental case presented is a process which is operating in Region A with constant process parameters. The second simulation and experimental case is a process which is operating in Region B with constant process parameters.

An important use for the LMD process is the repair of high-value parts. In these operations, material may be removed from the part to be repaired in a fashion such that the resulting substrate is non-uniform, i.e., corroded sections are removed while non-corroded sections are left untouched. The result of this operation may result in an uneven substrate onto which the repair is made. In order to simulate this, a portion of the substrate has been machined to leave a pocket 0.600 mm deep by 25.4 mm long. A photograph of substrate and pocket used in the experimental cases is shown in Figure 5.



Figure 5. Photograph of substrate and pocket feature used in experimental cases.

The simulations are seeded with this feature as the initial condition for part height. The model parameters are given in Table 1 and the process parameters are listed in Table 2. Figure 6 shows the location of the two operating points, along the $\lambda = 1.8 \times 10^{-5}$ kg/mm contour, on the process map. For Case 1, the stable build, $\kappa_2 = 4.570 \times 10^{-2}$. For Case 2, $\kappa_2 = -4.950 \times 10^{-2}$ indicating an unstable build. The only difference between the two build cases is the part standoff distance.

Table 2. Process parameters used for cases.

| Process Parameter | Case 1 (Stable) | Case 2 (Unstable) |
|--------------------------------------|-------------------|-------------------|
| Bead Height, δh (mm) | 0.381 | 0.381 |
| Spatial Flow Rate, λ (kg/mm) | 1.878×10 | 1.878×10 |
| Part Standoff Distance, d_p (mm) | 9.808 | 11.396 |

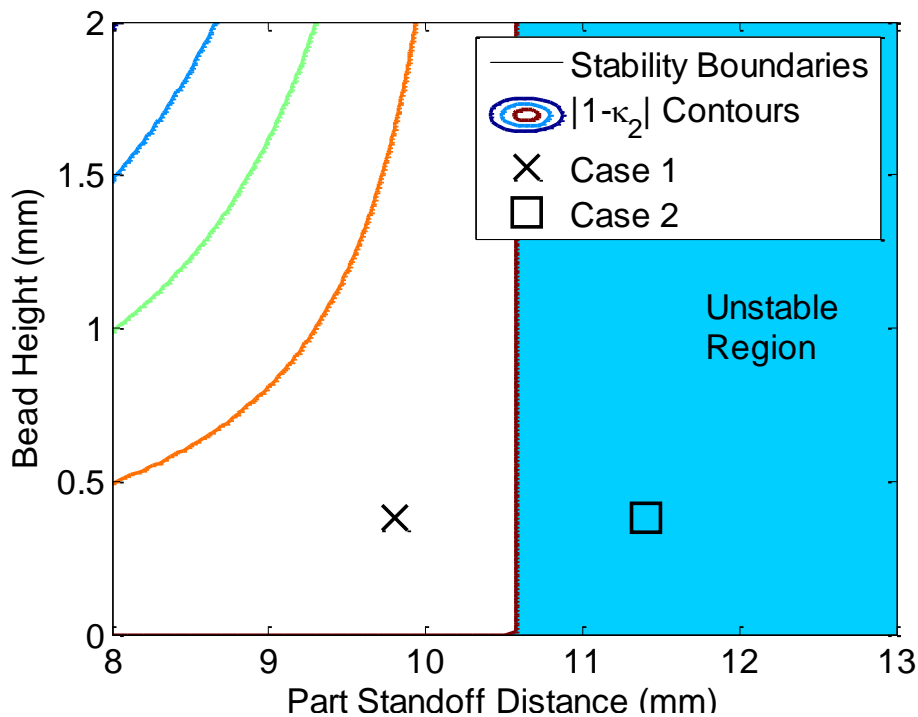


Figure 6. Process map with operating points for Cases 1 and 2 labeled.

The top pane in Figure 7 shows the simulated part height for Case 1 at every third layer from layer $j = 1$ to $j = 24$. As evidenced by the height profiles in Figure 7, because the process is layer-to-layer stable, the perturbations from equilibrium caused by the initial pocket in the substrate are attenuated each layer and after approximately layer $j = 15$, all evidence of the initial pocket is gone and each layer has a uniform bead height. Using the same process parameters, a 316 Stainless Steel thin-walled part was deposited on a steel substrate with a pocket 0.6 mm deep and 25.4 mm long using an Optomec LENS system. A photograph of the resulting deposition is shown in the bottom pane in Figure 7. The qualitative behavior of the deposition and the simulation are in very good agreement.

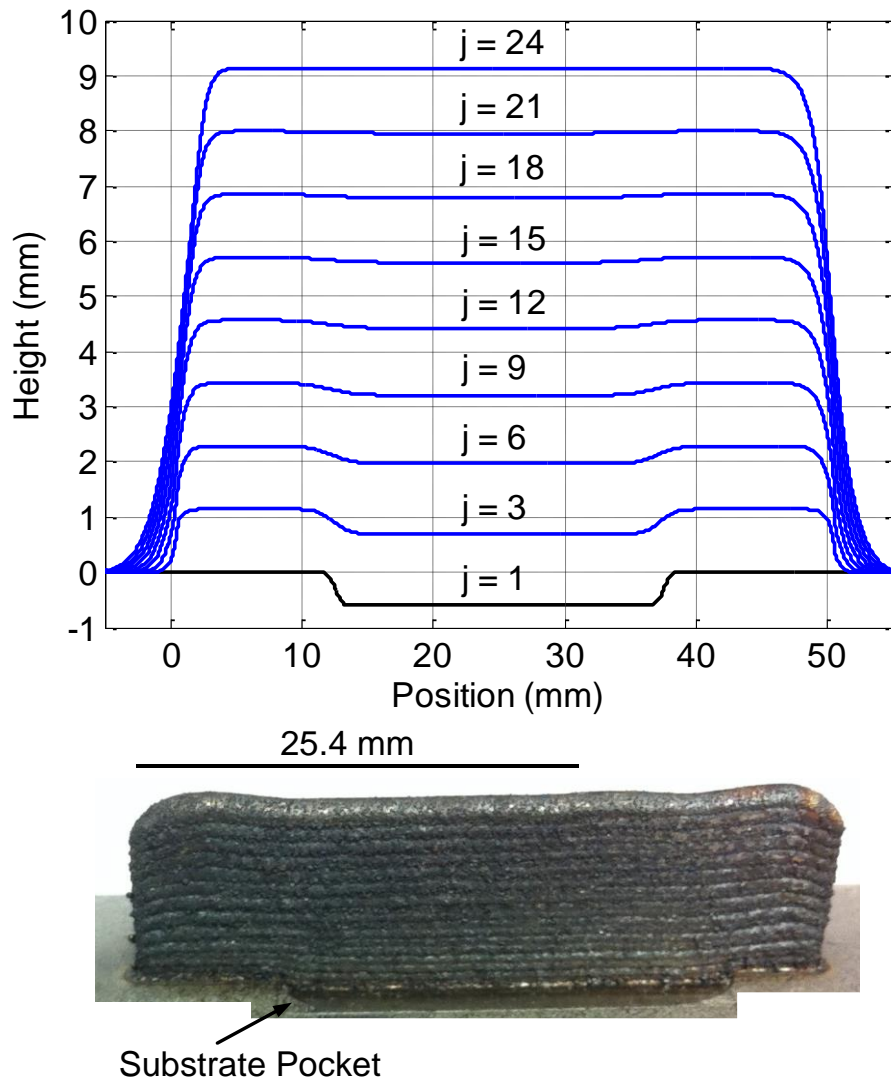


Figure 7. Simulation height signals for every third layer for $j = 1$ to $j = 24$ and photograph of the experimental deposition for stable Case 1.

Figure 8 shows the simulated and experimental results for Case 2 where the open-loop process is unstable. While the simulation and experimental depositions start out in a very similar fashion to Case 1 where the open-loop process is stable, the taller features quickly outpace the build rate of the lower features resulting in the large U-shaped defect in the final part. This unstable deposition would either require much earlier operator intervention to move the operating point into the stable region or the taller features would need to be machined off and the deposition restarted.

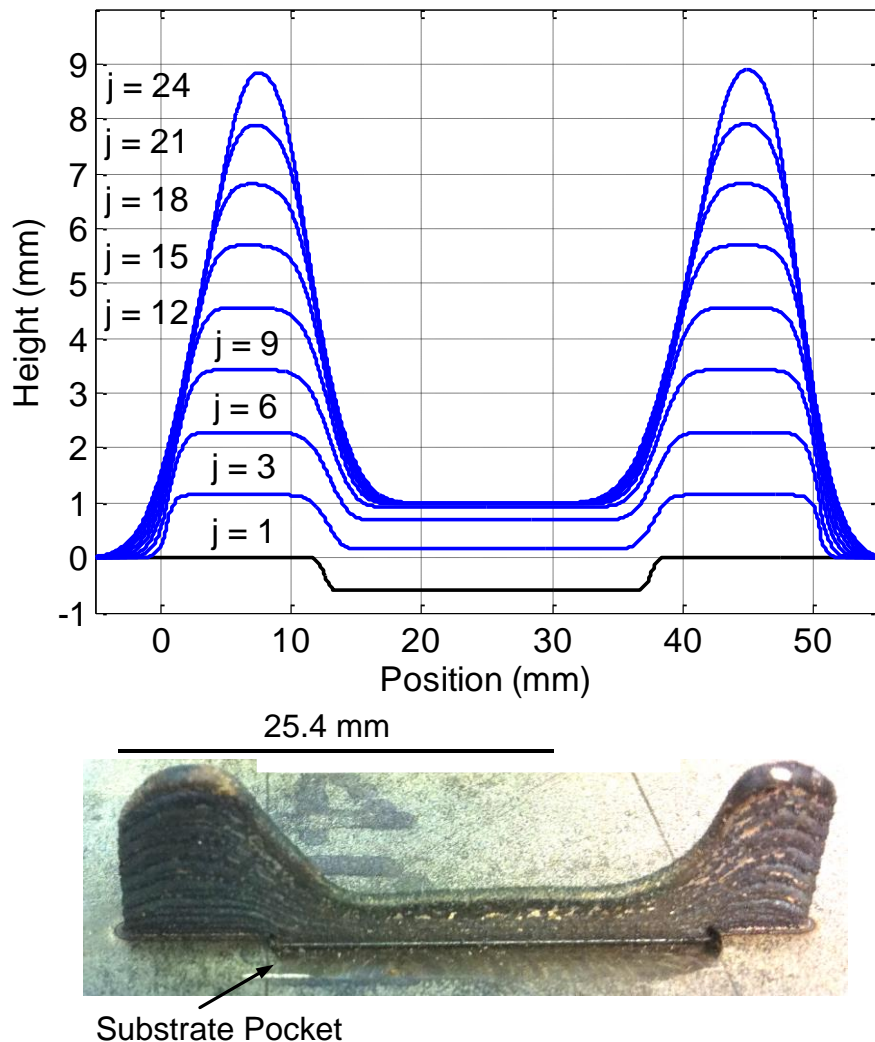


Figure 8. Simulation height signals for every third layer for $j = 1$ to $j = 24$ and photograph of the experimental deposition for stable Case 2.

Summary and Conclusions

The LMD process is an important process for the creation of one-off functional metal components and the repair of high-value parts. In contrast to how it is typically modeled, the LMD process possesses dynamics both within the layer and from layer-to-layer. Because of this, ostensibly valid choices for process parameters can result in failed builds.

A two-dimensional repetitive process model of the LMD process is presented which enables the application of repetitive process control theory to develop a DC-gain condition for the stability of LMD fabrications. The criterion is explicitly dependent on the slope of the powder catchment efficiency function. Because the criterion is a function of process inputs, process maps can be generated for specific processes to determine the regions of stability in the process parameters space. The map could enable operators to quickly tune or plan their process builds without the need for extensive testing. Simulation and experimental results of two

operating points – one stable and one unstable – indicate that the process map is effective in predicting the stable and unstable behavior of multi-layer LMD fabrications.

Acknowledgements

This work was supported in part by the National Science Foundation (CMMI1301414) and through a US Department of Education GAANN Fellowship (P200A120062), with technical and experimental support from Optomec and MachMotion.

References

- [1] Doumanidis, C. and Kwak, Y-M., 2001, “Geometry Modeling and Control by Infrared and Laser Sensing in Thermal Manufacturing with Material Deposition,” *ASME Journal of Manufacturing Science and Engineering*, vol. 123, no. 1, pp. 45–52.
- [2] Pinkerton, A. and Li, L., 2004, “Modelling the Geometry of a Moving Laser Melt Pool and Deposition Track via Energy and Mass Balances,” *Journal of Physics D: Applied Physics*, vol. 37, no. 14, pp. 1885-1895.
- [3] Tang, L. and Landers, R.G., 2010, “Melt Pool Temperature Control for Laser Metal Deposition Processes, Part I: Online Temperature Control,” *ASME Journal of Manufacturing Science and Engineering*, vol. 132, no. 1, pp. 011010:1-9.
- [4] Sammons, P.M., Bristow, D.A., Landers, R.G., 2014, “Control-Oriented Modeling of Laser Metal Deposition as a Repetitive Process,” *American Control Conference*, Jun 4-6th, Portland, OR.
- [5] Rogers, E., Galkowski, K., Owens, D.H., *Control Systems Theory and Applications for Linear Repetitive Processes*, Berlin, Springer, 2007.
- [6] Sammons, P.M., Bristow, D.A., Landers, R.G., 2014, “Frequency Domain Identification of a Repetitive Process Control Oriented Model for Laser Metal Deposition Processes,” *International Symposium on Flexible Automation*, July 14-16th, Awaji Island, Hyogo, Japan.
- [7] “LENS MR-7 Systems – Optomec Additive Manufacturing,” *Optomec Additive Manufacturing*, Web, 10 July 2015.